Kinetics and Mechanisms of Charge-transfer Nitration. Part 2.[1] Time-resolved Spectral Evolution of the *ipso* Adducts from 1,4-Dimethylnaphthalene Cation Radical

S. Sankararaman and J. K. Kochi *
Department of Chemistry, University of Houston, University Park, Houston, TX 77204-5641, USA

The transient intermediates accompanying the charge-transfer excitation of the 1,4-dimethylnaphthalene (DMN) complex with either the *N*-nitropyridinium or tetranitromethane acceptor are identified as the cation radical $DMN^{+\bullet}$ paired with NO_2 and either pyridine or trinitromethanide. Time-resolved (ps and ns–μs) spectroscopy allows the temporal evolution of these triads of reactive intermediates to the *ipso* adducts **1** and **2** to be followed in detail and the mechanistic relationship to nuclear and sidechain (methyl) nitration is delineated. The role of added pyridine bases in the promotion of sidechain nitration is discussed.

The efficient nitration of naphthalene and its methylated analogues was shown in the foregoing study[1] to occur upon the deliberate photo-excitation of the charge-transfer absorption bands of the precursor (EDA) complexes with various nitro-containing acceptors (NO_2–X). Particularly relevant was the formation of the *ipso* adducts **1** and **2** as the metastable, but isolable, intermediates in the sidechain nitration of 1,4-dimethylnaphthalene (DMN) from the tetranitromethane [X = $C(NO_2)_3^-$] and *N*-nitropyridinium (X = pyridine) complexes, respectively. Importantly, the adducts **1** and **2** in *charge-transfer nitration* are directly related to the transient *ipso* adducts **4** reported earlier by Fischer and Wilkinson in the electrophilic (thermal) nitration of DMN at −40 °C with nitric acid in acetic anhydride,[2] eqn. (1), in which the efficient trapping of the Wheland intermediate **3** occurred with the nucleophilic species (X = nitrate and acetate) extant in the nitration medium. Since the formation of such structurally related *ipso* intermediates as **1**, **2** and **4** suggests that charge-transfer (CT) nitration bears directly on electrophilic aromatic nitration,[3] particularly with regard to electron-transfer activation,[4] it is important to establish the kinetic behaviour of the pertinent ion-radical pair derived from the 1,4-dimethylnaphthalene donor (DMN). Accordingly, in the present study, we focussed our attention on the fate of [$DMN^{+\bullet}$, NO_2] as it evolved into the *ipso* adducts **1** and **2**, and to the nuclear/sidechain nitration of 1,4-dimethylnaphthalene. To this end, we proceeded from our previous time-resolved spectroscopic studies of tetranitromethane complexes with aromatic donors (ArH),[5,6] in which the spontaneous formation of the relevant cation-radical pair by charge-transfer excitation ($h\nu_{CT}$) was established as shown in Scheme 1.

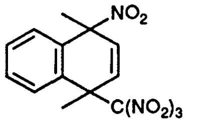

1

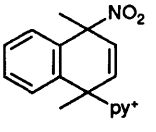

2

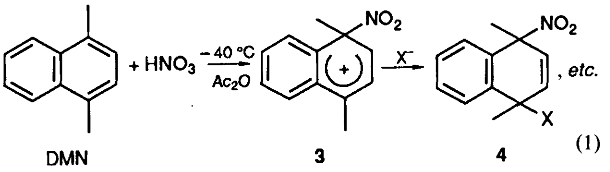

$$ArH + C(NO_2)_4 \rightleftharpoons [ArH, C(NO_2)_4] \qquad (2)$$

$$[ArH, C(NO_2)_4] \xrightarrow{h\nu_{CT}} [ArH^{+\bullet}, NO_2, C(NO_2)_3^-] \qquad (3)$$

Scheme 1

In Scheme 1, the reactive ion-radical intermediates $ArH^{+\bullet}$ and NO_2 are born within < 3 ps as the intimate ion-radical pair, initially trapped within the solvent cage (indicated by the brackets).[7] As applied to the 1,4-dimethylnaphthalene donor pertinent to the *ipso* adducts **1** and **2**, our initial task was to establish the CT formation of the cation-radical $DMN^{+\bullet}$ spectroscopically, and then to follow its disappearance under the conditions outlined above.

Results and Discussion

When a colourless solution of *N*-nitropyridinium tetrafluoroborate in acetonitrile was added to an excess of 1,4-dimethylnaphthalene (DMN), the solution turned bright brown. The absorption spectrum in Fig. 1(*a*) shows the appearance of the partially resolved absorption band of the charge-transfer complex, with λ_{CT} = 425 nm, eqn. (4).

$$DMN + pyNO_2^+ \overset{K}{\rightleftharpoons} [DMN, pyNO_2^+] \qquad (4)$$

Similarly, the exposure of DMN to the tetranitromethane (TNM) acceptor also resulted in a bright yellow solution, but the charge-transfer band appeared as a long tail absorption in the 350–550 nm spectral region. Although no distinctive absorption maximum was discerned, Fig. 1(*b*) clearly shows λ_{CT} to lie under the local absorptions of the donor and acceptor. Such a blue-shift of the charge-transfer band of the tetranitromethane complex of DMN, relative to that of the *N*-nitropyridinium complex, is in accord with the better acceptor properties of $pyNO_2^+$ compared with $C(NO_2)_4$, as indicated by their reduction potentials of E_p = +0.10 and −0.03 V *vs.* SCE, respectively.[8] The association constants *K* in eqns. (4) and (5)

$$DMN + C(NO_2)_4 \overset{K}{\rightleftharpoons} [DMN, C(NO_2)_4] \qquad (5)$$

were evaluated by the absorbance change at the monitoring wavelength, λ_{mon} = 450 nm, with increasing concentrations of the DMN donor, according to the Benesi–Hildebrand procedure.[9] The limited magnitudes of $K = 0.92\ dm^3\ mol^{-1}$ ($\varepsilon = 212\ dm^3\ mol^{-1}\ cm^{-1}$) and $0.23\ dm^3\ mol^{-1}$ ($\varepsilon = 288\ dm^3$

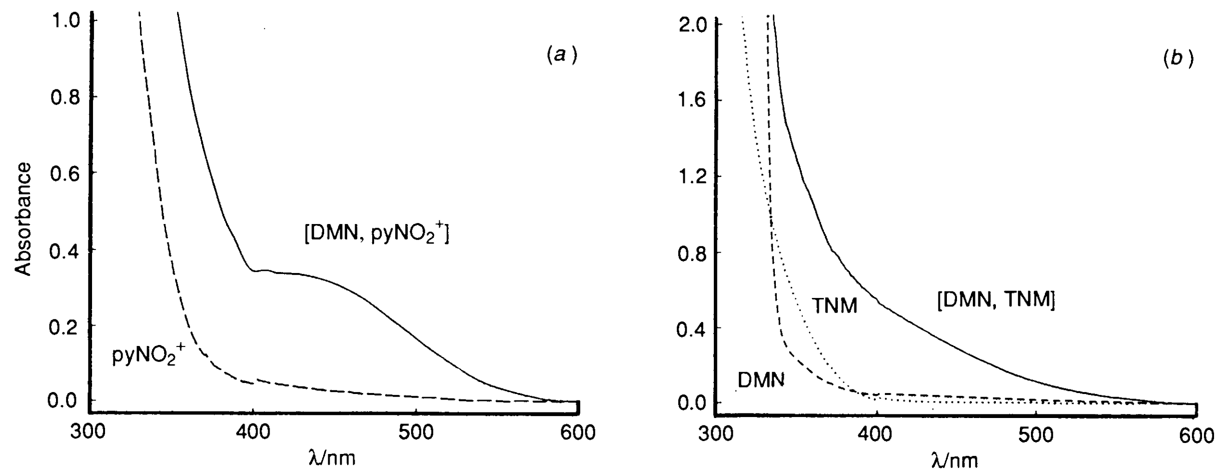

Fig. 1 Charge-transfer spectra of the DMN complexes with (*a*) the *N*-nitropyridium and (*b*) the tetranitromethane acceptors in relation to the absorption spectra of the uncomplexed DMN donor and $pyNO_2^+$/ $C(NO_2)_4$ acceptors in acetonitrile

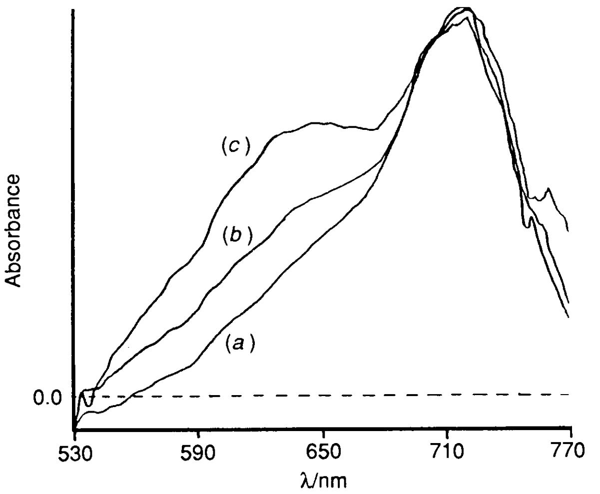

Fig. 2 Time-resolved (ps) absorption spectrum of $DMN^{+\bullet}$ at (*a*) 20, (*b*) 300 and (*c*) 980 ps, following the charge-transfer excitation, at 532 nm, of the DMN complex with tetranitromethane in dichloromethane, showing the growth of $(DMN)_2^{+\bullet}$ with λ_{max} = *ca.* 650 nm

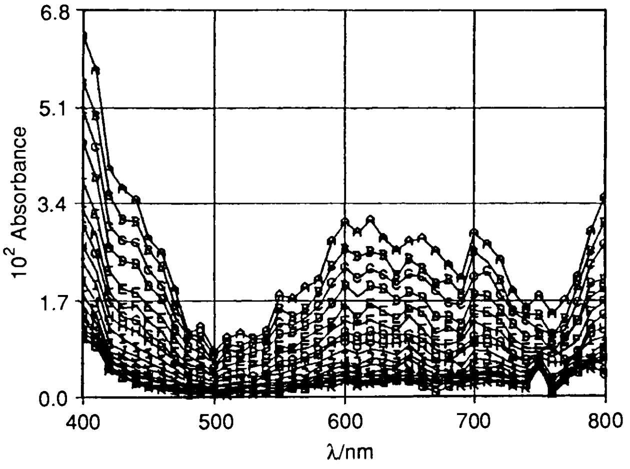

Fig. 3 The decay of the spectral transient in the time interval of 700 ns to 1 μs, following the laser flash excitation, at 532 nm, of the DMN complex with tetranitromethane in dichloromethane

mol^{-1} cm^{-1})[1] indicate that the DMN complexes with the *N*-nitropyridinium and tetranitromethane acceptors are both to be classified as weak.[10,11]

Time-resolved Spectroscopic Studies of the 1,4-*Dimethylnaphthalene Cation Radical by Charge-transfer Excitation.*—(*a*) *From the DMN complex with tetranitromethane.* The photobleaching of the CT band in Fig. 1(*b*) was examined by time-resolved spectroscopy in two time regimes. Thus the laser excitation of the DMN complex was carried out at λ_{exc} = 532 nm, initially with the 30 ps pulse derived from the frequency-doubled output of a mode-locked Nd^{3+}:YAG oscillator. This excitation pulse clearly corresponded to only the low-energy tail of the CT absorption band. Thus there was no ambiguity about either the adventitious local excitation of the uncomplexed 1,4-dimethylnaphthalene (DMN)[12] or tetranitromethane (TNM),[13] or the generation of intermediates which did not result from the direct charge-transfer excitation of the [DMN, TNM] complex. When the CT excitation with the laser pulse was carried out under conditions relevant to the charge-transfer nitration[1] (*e.g.*, 0.10 mol dm^{-3} DMN and 0.28 mol dm^{-3} tetranitromethane in acetonitrile), an intense absorption in the visible region between 600 and 750 nm was observed within the risetime (30 ps fwhm) of the laser pulse. The transient absorption band with λ_{max} = 710 nm, with a slight shoulder at *ca.* 650 nm, in Fig. 2 corresponded to the visible spectrum of the cation radical of 1,4-dimethylnaphthalene ($DMN^{+\bullet}$) previously generated from the corresponding tropylium and osmium tetraoxide complexes.[14,15] Moreover this spectral assignment was consistent with that reported for the parent naphthalene cation radical $NP^{+\bullet}$, with λ_{max} = 700 nm, by Brocklehurst,[16] and Steenken and co-workers.[17] At longer time delays (400 ps to 1 ns), the absorbance at *ca.* 650 nm gradually increased, until it appeared with a partially resolved maximum at λ = 640 nm (see Fig. 2). The latter was scrutinized more carefully in the ns–μs time regime by carrying out the laser excitation of the [DMN, TNM] complex at λ_{exc} = 532 nm with 10 ns pulses from a Q-switched Nd^{3+}:YAG laser. Thus the charge-transfer excitation of a solution containing 0.1 mol dm^{-3} 1,4-dimethylnaphthalene and 0.28 mol dm^{-3} tetranitromethane in acetonitrile produced a transient intermediate, the absorption spectrum of which is shown in Fig. 3. The visible absorption in the 550–750 nm region can readily be assigned to the dimer cation radical of 1,4-dimethylnaphthalene. For comparison, the visible absorption spectrum of $(DMN)_2^{+\bullet}$ in aqueous perchloric acid at pH 2 (obtained by means of the pulse radiolytic method)[18] consisted of broad absorption in the region 560–750 nm with maxima at 660, 690 and 720 nm. Furthermore, the visible absorption spectrum of the dimer cation radical of the parent naphthalene $(NP^{+\bullet})_2$, with λ_{max} = 580 nm, is deduced from the spectral data reported in the

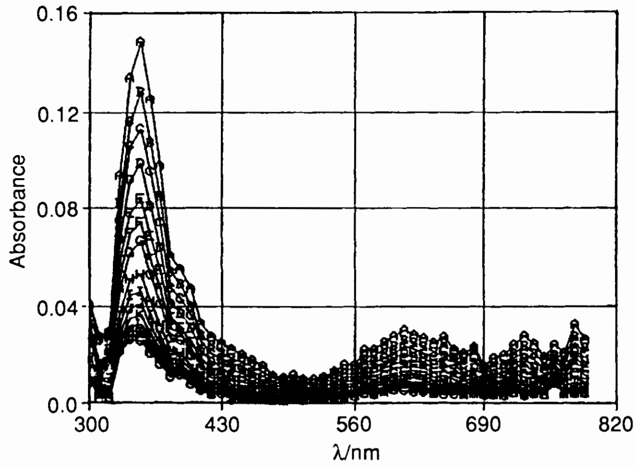

Fig. 4 Time-resolved μs absorption spectrum from the charge-transfer excitation of 0.2 mol dm^{-3} DMN and 0.02 mol dm^{-3} TNM in dichloromethane, showing the well-resolved band of trinitromethanide (λ_{max} = 350 nm)

literature.[16,19–21] [Note the dimer cation radical of naphthalene also shows a broad near-IR absorption at λ_{max} = *ca.* 1200 nm.[17]]

The temporal evolution of the dimethylnaphthalene cation radical to the dimer cation radical from the ps to μs time regimes in Figs. 2 and 3 corresponds to the second-order rate constant of $k_a \sim 10^8$ dm^3 mol^{-1} s^{-1} evaluated independently[17] in eqn. (6).

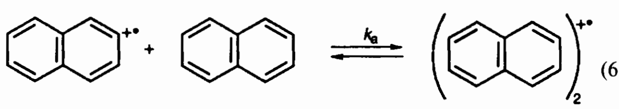

(6)

Such a facile π-association of aromatic cation radicals has been generally observed with various arene donors,[22] and a reversible association constant of K = 50 mol^{-1} dm^3 has been evaluated for anthracene in dichloromethane.[23] The time-resolved spectroscopic studies thus establish the charge-transfer activation of the DMN complex with tetranitromethane to proceed as shown in Scheme 2. Ar represents DMN and related

$$\mathrm{Ar} + \mathrm{C(NO_2)_4} \overset{K}{\rightleftharpoons} [\mathrm{Ar}, \mathrm{C(NO_2)_4}] \qquad (7)$$

$$[\mathrm{Ar}, \mathrm{C(NO_2)_4}] \xrightarrow[(\mathrm{ps})]{h\nu_{\mathrm{CT}}} [\mathrm{Ar}^{+\bullet}, \mathrm{NO_2}, \mathrm{C(NO_2)_3}^-] \qquad (8)$$

$$[\mathrm{Ar}^{+\bullet}, \mathrm{NO_2}, \mathrm{C(NO_2)_3}^-] + \mathrm{Ar} \xrightarrow[(\mathrm{ns}\text{–}\mu\mathrm{s})]{} \mathrm{Ar_2}^{+\bullet} + \mathrm{NO_2} + \mathrm{C(NO_2)_3}^- \qquad (9)$$

Scheme 2

aromatic donors. The observation of NO_2 was somewhat obscured by the spectral overlap of its weak, broad continuum (spanning the spectral region from 250 to > 800 nm[24]) with the strong local absorptions of the aromatic donor and its cation radical. As such, the presence of NO_2 may be surmised as the weak pervasive background absorbance in both the ps and μs transient spectra.[7] The transient (visible) spectrum of $(DMN)_2^{+\bullet}$ shown in Fig. 3 was obtained from the photoexcitation, at λ_{exc} = 532 nm, of a solution of 0.05 mol dm^{-3} 1,4-dimethylnaphthalene and 0.16 mol dm^{-3} tetranitromethane in dichloromethane with the 10 ns laser pulse. The wider spectral window allowed by the photoexcitation of a solution containing inverted concentrations of 0.16 mol dm^{-3} DMN and 0.05 mol dm^{-3} TNM [to minimize the high background absorption of TNM in Fig. 1(*b*)] shows the simultaneous presence of $(DMN)_2^{+\bullet}$, as well as trinitromethanide with λ_{max} = 350 nm

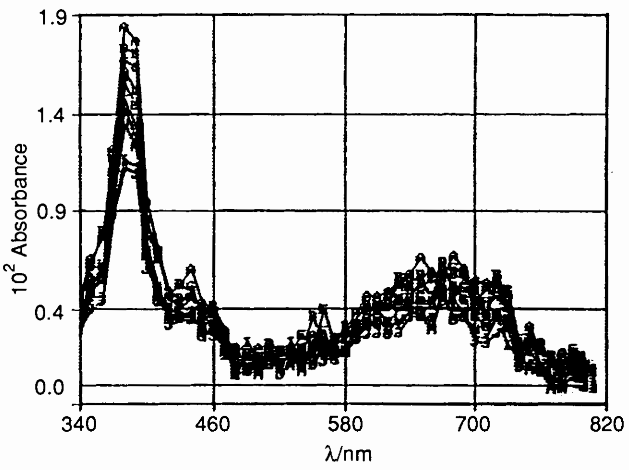

Fig. 5 The transient absorption spectrum of $(DMN)_2^{+\bullet}$ from the charge-transfer excitation, at 532 nm, of the *N*-nitropyridinium complex with DMN in acetonitrile

(ε = 14 000 dm^3 mol^{-1} cm^{-1}),[7] in Fig. 4. Similar transient absorption spectra were obtained in acetonitrile and in methanol, except that the broad band at 550–750 nm was red-shifted by *ca.* 20 nm in these polar solvents.

(*b*) *From the DMN complex with the* N-*nitropyridinium acceptor.* The EDA complexes of aromatic donors with $pyNO_2^+BF_4^-$ have visible absorptions [Fig. 1(*a*)] suitable for charge-transfer excitation at 532 nm. The photoexcitation of the 1,4-dimethylnaphthalene complex was successfully carried out at λ_{exc} = 532 nm to produce the transient absorption spectrum shown in Fig. 5. This spectrum coincides with the transient absorption spectrum of $(DMN)_2^{+\bullet}$ in Fig. 4, obtained from the charge-transfer excitation of the dimethylnaphthalene complex with tetranitromethane. [Note that the higher energy bands with λ_{max} = 380 and 440 nm appear as a pair of unresolved shoulders on the trinitromethanide absorption in Fig. 4.] Similar transient absorption spectra were observed in the photoexcitation of the *N*-nitropyridinium complexes with other aromatic donors such as hexamethylbenzene ($HMB^{+\bullet}$ with λ_{max} = 480 nm),[25] and 9-methyl- and 9,10-dimethyl-anthracenes ($MA^{+\bullet}$ and $DMA^{+\bullet}$ with λ_{max} centred at 640 and 680 nm).[26] The accompanying *N*-nitropyridinyl radical ($pyNO_2^{\bullet}$) was not identified directly. However, the separate transient electrochemical studies at cyclic voltammetric sweep rates exceeding 10^5 V s^{-1} failed to detect chemical reversibility in the *N*-nitropyridinium reduction.[8] Accordingly, the lower limit of τ < 1 μs for the lifetime for $pyNO_2^{\bullet}$ in its dissociation to pyridine and NO_2, coupled with the facile π-dimerization of $DMN^{+\bullet}$, suggests that the charge-transfer activation of the *N*-nitropyridinium complexes effectively proceeds in the same manner as that for the tetranitromethane complex (Scheme 3).

$$\mathrm{Ar} + \mathrm{pyNO_2}^+ \rightleftharpoons [\mathrm{Ar}, \mathrm{pyNO_2}^+] \qquad (10)$$

$$[\mathrm{Ar}, \mathrm{pyNO_2}^+] \xrightarrow{h\nu_{\mathrm{CT}}} [\mathrm{Ar}^{+\bullet} + \mathrm{NO_2} + \mathrm{py}] \qquad (11)$$

$$[\mathrm{Ar}^{+\bullet}, \mathrm{NO_2}, \mathrm{py}] + \mathrm{Ar} \longrightarrow \mathrm{Ar_2}^{+\bullet}, \mathrm{NO_2}, \mathrm{py} \qquad (12)$$

Scheme 3

The time-resolved spectral studies thus show that $(DMN)_2^{+\bullet}$ is the predominant species in the temporal relaxation of the 1,4-dimethylnaphthalene cation radical to the μs time regime. However, the *rate* of its reversible dissociation is likely to be rapid, irrespective of the magnitude of K in eqn. (6).[22] [For example, a rate constant for dissociation of $k_d > 10^6$ s^{-1} can be estimated from the value of $K < 10^2$ mol^{-1} dm^3 and k_a = *ca.* 10^8 mol^{-1} dm^3 s^{-1} in eqn. (6).[17,23]]

Table 1 Salt effect on the decay kinetics of the spectral transient in dichloromethane[a]

Additive[b]	Concentration/mol dm^{-3}	Kin. order[c]	Rate constant[d]
None	—	2	2.0×10^7
TBAP	0.005	2	2.5×10^6
TBAP	0.01	2	1.5×10^6
TBAP	0.015	2	1.2×10^6
TBAP	0.02	2	1.0×10^6
TBAP	0.04	2	9.4×10^5
TBAP	0.06	2	6.8×10^5
TBAP	0.08	2	7.2×10^5
TBAP	0.1	2	6.9×10^5
TBAP	0.2	2	6.2×10^5
TBAT	0.05	1	7.6×10^5
TBAT	0.10	1	7.5×10^5

[a] From the CT excitation at 532 nm of 0.05 mol dm^{-3} DMN and 0.16 mol dm^{-3} TNM in dichloromethane. [b] TBA = tetrabutylammonium, P = perchlorate, T = trinitromethanide. [c] Kinetic order as monitored at λ_{mon} = 625 nm: 2 = second-order, 1 = first-order. [d] First- and second-order rate constants in units of s^{-1} and A^{-1} s^{-1}, respectively (A = absorbance unit).

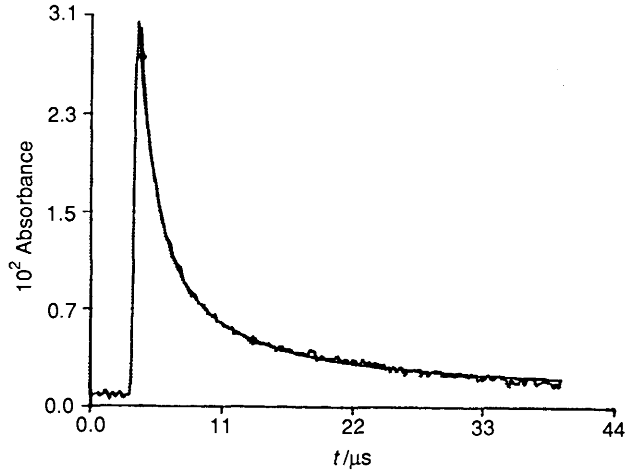

Fig. 6 The disappearance of the spectral transient, at λ_{mon} = 625 nm, following the CT excitation of the DMN complex with tetranitromethane in dichloromethane. The fit to second-order kinetics is shown by the computer-generated smooth line with $k_2 = 2 \times 10^7$ A^{-1} s^{-1}.

Temporal Evolution of the 1,4-*Dimethylnaphthalene Cation Radical*.—The spontaneous generation of the cation radical pair from the charge-transfer excitation of the tetranitromethane and *N*-nitropyridinium complexes with 1,4-dimethylnaphthalene, according to Schemes 2 and 3, allowed their subsequent disappearance to be followed by monitoring spectral transients, typically shown in Figs. 3 and 4. Before proceeding however, it is important to emphasize that the quantitative accounting of all products from the charge-transfer nitration carried out under the same conditions [1] establishes the stoichiometric fate of each species included in the brackets in Schemes 2 and 3. For example, the decay kinetics in dichloromethane solutions relate directly to the conditions extant in the steady-state photolysis to produce essentially quantitative yields of the *ipso* adduct **1**,[1] eqn. (13). On the other hand, the photoexcitation of the same tetranitromethane complex of DMN in acetonitrile afforded a three-product mixture, eqn. (14), the composition of which was temperature dependent.[1]

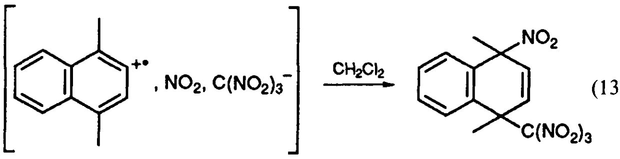

(13)

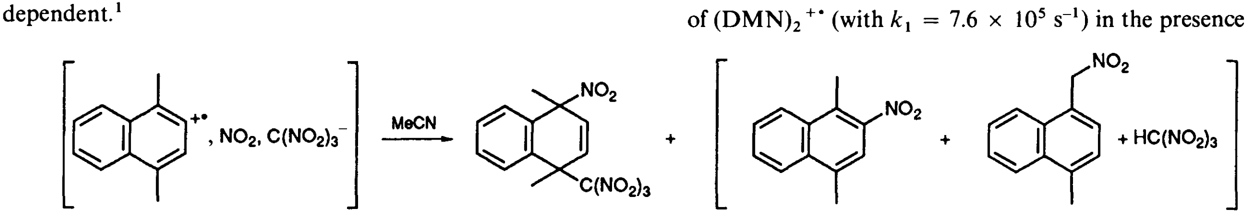

(14)

In order to delineate the different pathways for the charge-transfer nitration, the decay of the spectral transient was scrutinized first in the dichloromethane [eqn. (13)] and then in acetonitrile [eqn. (14)]. Although the reactivities of aromatic cation radicals and their π-dimers differ,[23] the following mechanisms can be considered in terms of either DMN$^{+\bullet}$ and/or (DMN)$_2^{+\bullet}$, owing to the facile dissociation (with expected $k_d > 10^6$ s^{-1}) in eqn. (6).

Ion-pair Annihilation to the ipso *Adduct* **1** *in Dichloromethane*.—The decay of the spectral transient in dichloromethane (Fig. 2) at the monitoring wavelengths of λ_{mon} = 430 and 625 nm showed no absorbance change up to 800 ns. However, at the slower µs timescale, in Figs. 3 and 4, the complete decay of the absorbance was noted, and it followed clean second-order kinetics, as shown by the fit of the data to the smooth line in Fig. 6 (which represents the computer-generated least-squares treatment of the data for second-order kinetics) all the way down to the baseline (*i.e.*, the complete disappearance of the spectral transient). The observed second-order rate constant of $k_2 = 2.0 \times 10^7$ A^{-1} s^{-1} (A = absorbance unit) is equivalent to the diffusion-controlled rate constant of $k_2 = 6 \times 10^{10}$ dm^3 mol^{-1} s^{-1} when the extinction coefficient of (DMN)$_2^{+\bullet}$ was taken as 3×10^3 dm^3 mol^{-1} cm^{-1}.[27,*] The second-order decay in Fig. 6 was confirmed by the invariance of k_2 with the decrease in (DMN)$_2^{+\bullet}$ concentration attendant upon the attenuation of the laser (excitation) pulse (see the Experimental section).

The magnitude of the second-order rate constant k_2 showed a marked dependence on the presence of added tetrabutylammonium perchlorate (TBAP), which is considered to be an inert salt.[28,†] Thus the presence of as little as 0.005 mol dm^{-3} TBAP was sufficient to decrease the value of k_2 by roughly an order of magnitude (Table 1). Furthermore, the effect of the common-ion salt tetrabutylammonium trinitromethanide (TBAT) was even more dramatic, causing a change in the kinetics from second-order to first-order. The first-order decay of (DMN)$_2^{+\bullet}$ (with $k_1 = 7.6 \times 10^5$ s^{-1}) in the presence of 0.05 mol dm^{-3} TBAT was also related to the first-order decay ($k_1 = 6.2 \times 10^6$ s^{-1}) observed when the tetranitromethane complex

---

[*] Based on the relative absorbances for the 1:1 molar ratios of (DMN)$_2^{+\bullet}$ and C(NO$_2$)$_3^-$ (ε 14 000 mol^{-1} dm^3 cm^{-1}) in Fig. 4.

[†] The magnitude of k_2 for DMN$^{+\bullet}$ in dichloromethane is roughly 10^2 times faster than that previously found for the more stabilized cation radicals derived from 9-phenyl- and 9,10-diphenyl-anthracene in the same solvent, but containing 0.2 mol dm^{-3} tetrabutylammonium hexafluorophosphate, by V. D. Parker and M. Tilset, *J. Am. Chem. Soc.*, 1987, **109**, 2521.

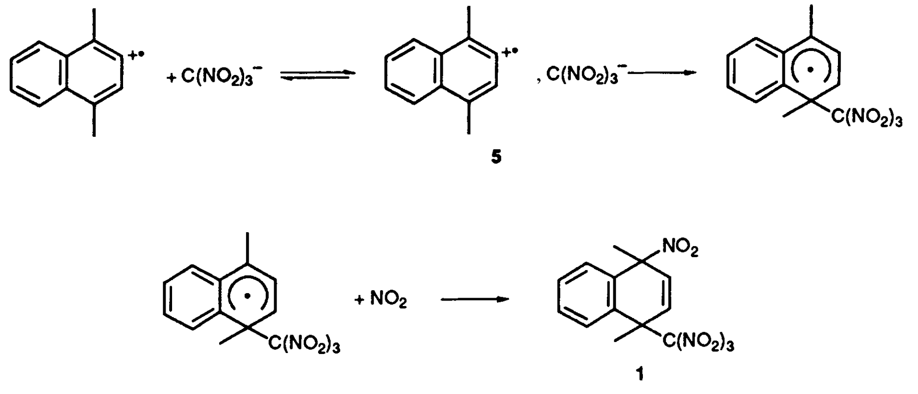

(15a,b)

(16)

Scheme 4

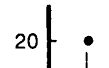

Fig. 7 Salt effect on the second-order rate constant, k_2, for the decay of the spectral transient shown in Fig. 3

of DMN was irradiated in the hydrocarbon solvent n-hexane. Such a drastic change in the kinetic order for the decay of the spectral transient, as effected by the solvent variation and added salt, was highly reminiscent of that previously observed in the unique behaviour of anthracene and anisole cation radicals under similar circumstances.[6,29] By direct analogy with the earlier studies, we attribute the second-order decay to the ion-pair annihilation of the trinitromethanide counterion formed in Scheme 2 with the dimethylnaphthalene cation radical at the *ipso* position (of highest charge density[30]). The subsequent coupling of the adduct radical with the residual NO_2 [see eqn. (13)] then constitutes the pathway for the formation of the *ipso* adduct **1**, eqns. (15a,b) and (16).*

The mechanistic formulation in Scheme 4 considers the ionic species to exist, in relatively non-polar solvents such as dichloromethane, as ion pairs,[31] which form the basis for the observed solvent and salt effects in the following manner.

(*a*) A solvent effect on the pre-equilibrium association of the ions in eqn. (15a) is consistent with the change in the decay kinetics to an overall first-order dependence when the photoexcitation of the tetranitromethane complex with DMN was carried out in hexane. Since the association of ions is complete in this hydrocarbon medium,[32] the adduct formation is determined solely by the first-order annihilation of the active ion pair **5** in eqn. (15b).

(*b*) The common-ion effect observed in the presence of added TBAT alters the second-order decay to first-order kinetics by converting all the free ions $(DMN)_2^{+\bullet}$ into the active ion pair **5**, eqn. (17). Such a formulation is in accord with the change to

$$(DMN)_2^{+\bullet} + Bu_4N^+C(NO_2)_3^- \rightleftharpoons (DMN)_2^{+\bullet}C(NO_2)_3^- + Bu_4N^+ \quad (17)$$

first-order kinetics in the presence of as little as 0.05 mol dm^{-3} TBAT. The results in Table 1 also show that the first-order rate constant obtained with added TBAT is independent of the salt concentration.[29]

(*c*) The special salt effect on the kinetic behaviour, in the presence of added TBAP, stands in strong contrast with the common-ion effect described above. The diminished second-order rate constant† now arises from the competitive scavenging of the active ion pair **5** by the inert salt, eqn. (18).

$$\underset{\text{(active ion pair)}}{(DMN)_2^{+\bullet}C(NO_2)_3^-} + Bu_4N^+ClO_4^- \rightleftharpoons \underset{\text{(inactive ion pair)}}{(DMN)_2^{+\bullet}ClO_4^-} + Bu_4N^+C(NO_2)_3^- \quad (18)$$

Such an ionic exchange effectively converts the chemically active ion pair **5** into an unreactive ion pair, which is kinetically akin to the dissociation into the free ion $(DMN)_2^{+\bullet}$.[29] The sharp drop-off in the observed second-order rate constant in Fig. 7 thus represents the partitioning of $(DMN)_2^{+\bullet}$ by the special salt effect to explain the high sensitivity of the ion-pair decay to the presence of otherwise inert salts.[6]

Radical-pair Collapse of the 1,4-*Dimethylnaphthalene Cation Radical with* NO_2 *in Acetonitrile*.—The spectral transient generated from the charge-transfer excitation of the tetranitromethane complex with DMN in acetonitrile, according to Scheme 2, persisted for a significantly longer period than that produced in dichloromethane. For example, the decay monitored at λ_{mon} = 625 nm was *ca.* 90% complete 270 μs after the laser flash, in acetontrile, compared with the complete decay of the transient to the base line within 9 μs in dichloromethane.

---

* For convenience, the subsequent mechanistic discussion will focus on the monomeric $DMN^{+\bullet}$ owing to its enchanced reactivity (compare ref. 23) and to the facile dissociation of the dimeric $(DMN)_2^{+\bullet}$ (note also that $k_d \leqslant k_1$ in hexane), as described above.

† According to Scheme 4, the observed second-order rate constants in Table 1 correspond approximately to Kk_1 where K is the ion-pair association constant and k_1 is the rate constant for the ion-pair annihilation in eqn. (15a,b).

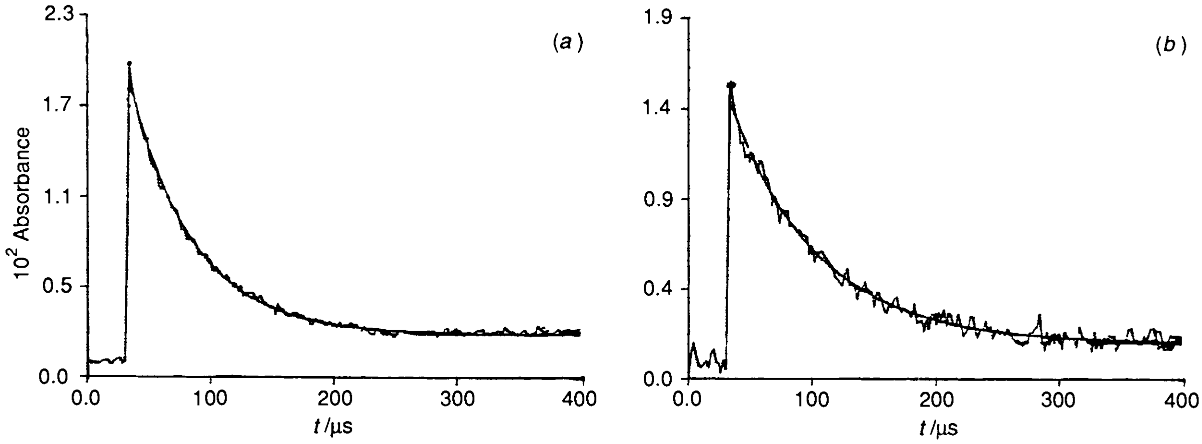

Fig. 8 (*a*) The decay of the spectral transient in acetonitrile for the CT excitation of the DMN complex with the tetranitromethane acceptor. The fit to first-order kinetics is shown by the computer-generated smooth line with $k_1 = 2 \times 10^4$ s^{-1}. (*b*) The same as (*a*) but with the *N*-nitropyridinium acceptor, with $k_1 = 1.5 \times 10^4$ s^{-1}.

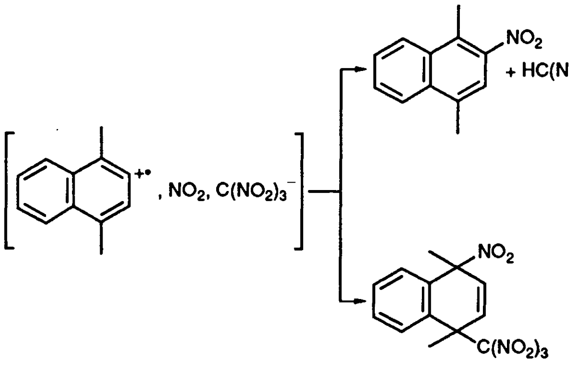

(19)

(20)

More significantly, the decay of the spectral transient in acetonitrile followed clean first-order kinetics, as shown by the unmistakable fit of the data to the computer-generated smooth curve in Fig. 8(*a*), with the first-order rate constant of $k_1 = 2.0 \times 10^4$ s^{-1}.

The different decay kinetics in dichloromethane and acetonitrile are also related to the distinctive products obtained from the charge-transfer nitration of 1,4-dimethylnaphthalene in these solvents. Thus the simultaneous nitration of DMN at the 2-position in acetonitrile [eqn. (14)] indicates that the triad formed in Scheme 2 disappears *via* two competing routes [eqns. (19) and (20)].* This is different from the single pathway in dichloromethane [eqn. (13)]. Ion-pair separation, which is more important in polar solvents such as acetonitrile,[33] accounts for the minor effect of added salts on the measured first-order rate constant.[29] We thus proceed from our earlier study of anisole cation radicals[6] to the *ipso* adduct *via* the first-order collapse of the radical-pair to the Wheland intermediate [eqn. (21)],† followed by ion-pair annihilation.

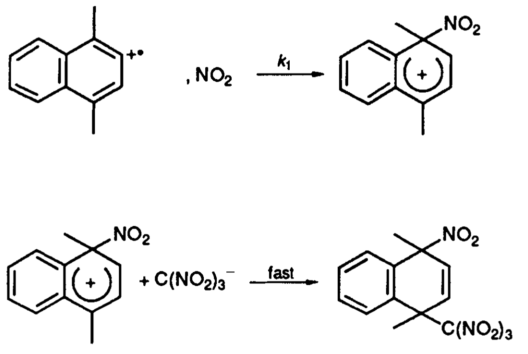

(21)

(22)

Scheme 5

According to this formulation, the nuclear nitration derives from the competitive collapse of the radical pair at the 2-position, which has the second highest electron density in the cation radical.[30]

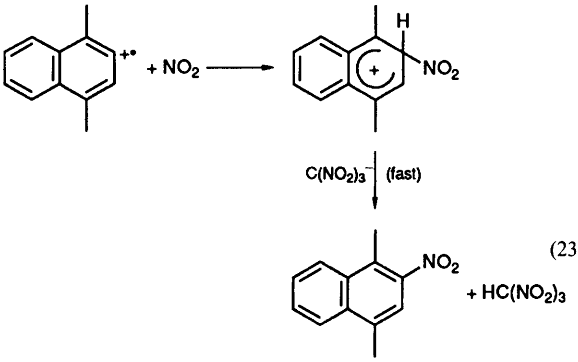

(23a,b)

The radical-pair collapse in eqn. (21) receives experimental support from the decay behaviour of the same spectral transient generated as the reactive intermediate from the charge-transfer activation of the *N*-nitropyridinium complex with DMN in Scheme 3. Thus Fig. 8(*b*) shows the formation of the *ipso* adduct **2** to occur via the first-order decay of the spectral transient (followed at $\lambda_{mon} = 650$ nm) with $k_1 = 1.5 \times 10^4$ s^{-1}, which is essentially the same as that obtained for the *ipso* adduct **1** from the tetranitromethane (*vide supra*). The coincident decays must involve a process common to both, eqn. (24), which is equivalent

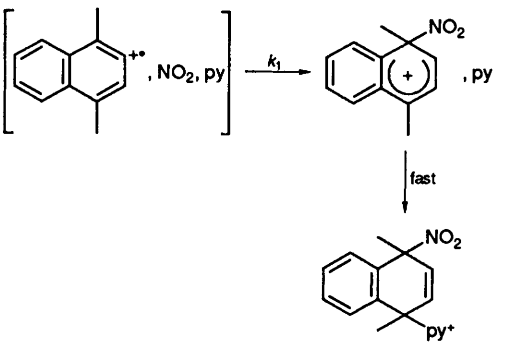

(24)

---

* The third component of the competition leading to sidechain nitration is discussed separately (*vide infra*).

† For details of the first-order decay of the radical pair in eqn. (21), see the previous study.[6]

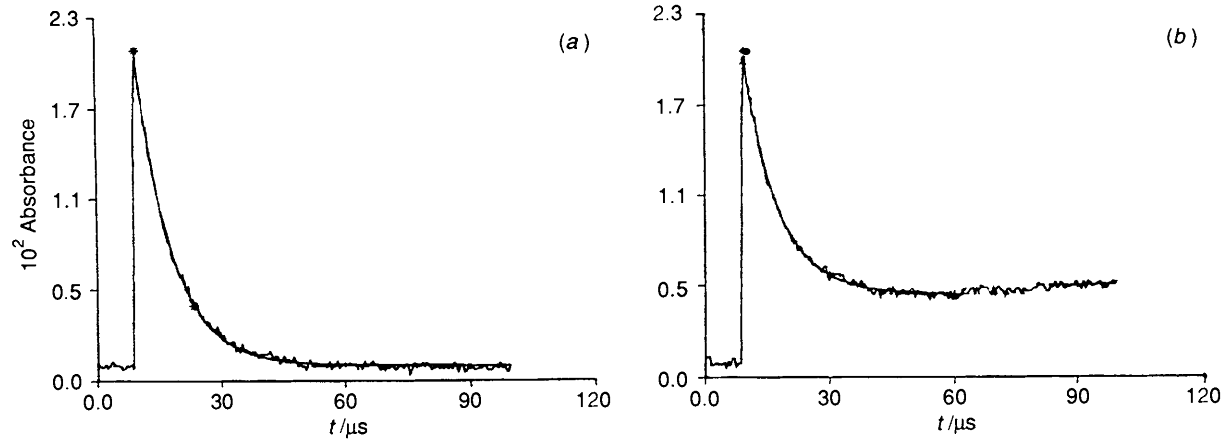

Fig. 9 (*a*) Effect of added base on the decay of the spectral transient (λ_{max} = 650 nm) from the CT excitation of the DMN complex with tetranitromethane in acetonitrile. The fit to first-order kinetics is shown by the fit of the computer-generated smooth line, with $k_1 = 1.20 \times 10^5$ s^{-1}. (*b*) Same as (*a*) but at λ_{mon} = 450 nm.

Table 2 Charge-transfer nitration of 1,4-dimethylnaphthalene in the presence of pyridine bases[a]

Nitronium carrier	T/°C	Additive	Nitration products (mol%) 2-NO$_2$	*ipso*[b]	SC[c]
$C(NO_2)_4$	25	None	9	43	40
$C(NO_2)_4$	0	None	8	65	23
$C(NO_2)_4$	0	DTBP[d]	13	9	62
$C(NO_2)_4$	0	Collidine	18	0	81
$pyNO_2^+BF_4^-$	0	None	1	70[e]	29

[a] In acetonitrile solution containing 0.1 mol dm^{-3} DMN and 0.5 mol dm^{-3} NO_2X at 0 °C. [b] *ipso* adduct **1**, unless indicated otherwise. [c] 1-Nitromethyl-4-methylnaphthalene **6**. [d] 2,6-Di-t-butylpyridine. [e] *ipso* adduct **2**.

to that in eqn. (21) of Scheme 5. On the other hand, the alternative pathway involving the nucleophilic addition of py to DMN$^{+\bullet}$ is expected to follow different kinetic behaviour since it corresponds to the second-order annihilation of the ions in eqn. (15) of Scheme 4.

Sidechain Nitration of 1,4-*Dimethylnaphthalene. Effect of Pyridine Bases*.—Charge-transfer nitration in acetonitrile solution also leads to the sidechain substitution of 1,4-dimethylnaphthalene [see eqn. (14)]. Since slightly higher yields of the sidechain-nitration product **6** were obtained from the photoexcitation of the *N*-nitropyridinium complexes compared with that obtained from the tetranitromethane complex,[1] the effect of added pyridine bases was examined. Indeed, the results in Table 2 show that significantly increased amounts of **6** were obtained in the presence of added 2,4,6-collidine and 2,6-di-t-butylpyridine as hindered, non-nucleophilic bases, eqn. (25).

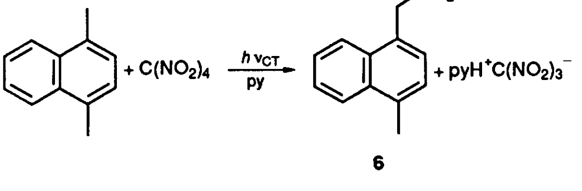

(25)

6

Table 3 Deprotonation of the 1,4-dimethylnaphthalene cation radical by added pyridine bases[a]

Solvent	Deprotonation $k_H/10^6$ mol^{-1} dm^3 s^{-1} [b] DTBP	Lutidine	Collidine
CH_2Cl_2	1.6	4.5	5.9 (1.4)
CH_3CN	—	1.3	2.7 (0.58)

[a] In solutions containing 0.05 mol dm^{-3} DMN, and 0.16 mol dm^{-3} TNM and excess base (see Fig. 10). [b] Determined under pseudo-first-order conditions at 25 °C, where DTBP = 2,6-di-butylpyridine. Numbers in parentheses for 1,4-[$^2H_6$]DMN.

The time-resolved spectroscopic studies of the photoexcitation of the tetranitromethane complex carried out in the presence of these added bases showed the same spectral transients as those present in Figs. 3 and 4. Notably different however, was the decay profile of the spectral transient monitored at λ_{mon} = 625 nm, which followed first-order kinetics ($k_1 = 1.20 \times 10^5$ s^{-1}) cleanly to the baseline [Fig. 9(*a*)]. The decay at λ_{mon} = 430 nm in Fig. 9(*b*) followed the same kinetics ($k_1 = 1.24 \times 10^5$ s^{-1}), but returned to *ca.* 75% of the initial absorbance owing to the residual absorption of the trinitromethanide ion (λ_{max} = 350 nm). The linear dependence of the pseudo-first-order rate constant k_1' on the concentration of the added pyridine is shown in Fig. 10.

The second-order rate constants evaluated from the slopes are listed as k_H in Table 3. The monotonic increase in the value of k_H with the base strength of the pyridine (py) is associated with the deprotonation of 1,4-dimethylnaphthalene cation radical, eqn. (26). The latter was confirmed by the deuterium kinetic isotope effect (KIE) that was evaluated with the methyl-labelled hexadeuterio derivative, 1,4-di[$^2H_3$]methylnaphthalene ([$^2H_6$]DMN),[34] under identical conditions. The values of the KIE with collidine in acetonitrile and dichloromethane were determined as k_H/k_D = 4.6 and 4.2, respectively, from the rate constants listed in Table 3. By comparison, the deuterium kinetic isotope effect for the deprotonation of hexamethylbenzene cation radical is k_H/k_D *ca.* 3.[35,36] The slightly lower value of the KIE for hexamethylbenzene accords with the lower stability of its cation radical relative to DMN$^{+\bullet}$, as indicated by the magnitudes of their oxidation potentials [HMB (1.65 V)[37] and DMN (1.5 V)].[38,*]

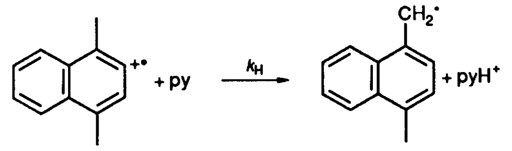

(26)

---

* Reversible oxidation potentials of arenes, E^0, in V *vs.* SCE. For a discussion of this point, see refs. 35 and 39.

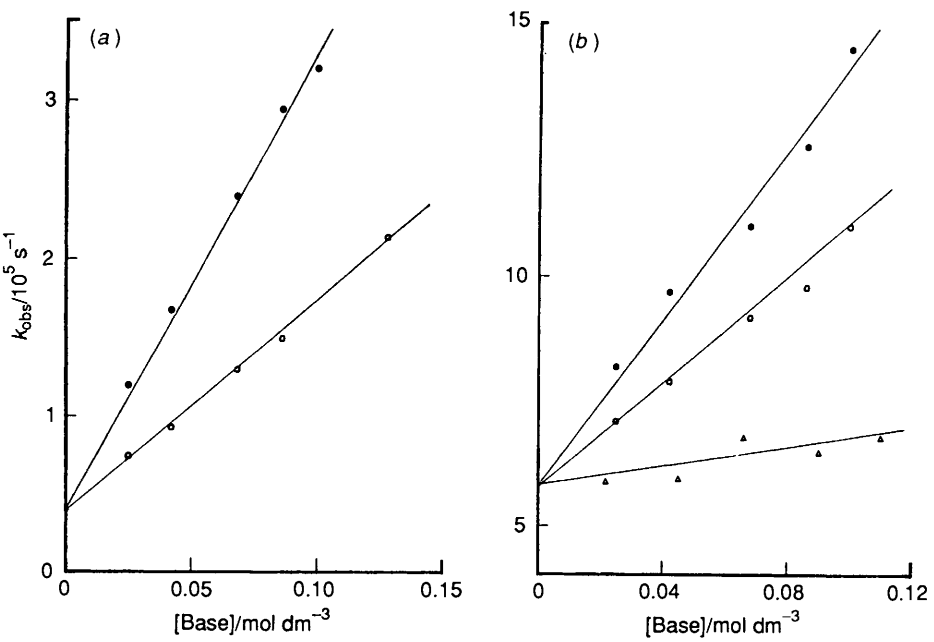

Fig. 10 Pseudo-first-order kinetics for the disappearance of the spectral transient from the CT excitation of the DMN complex with TNM in the presence of added (*a*) 2,4,6-collidine (●) and 2,6-lutidine (○) in acetonitrile, and (*b*) 2,6-lutidine (○), 2,4,6-collidine (●) and 2,6-di-t-butylpyridine (△) in dichloromethane

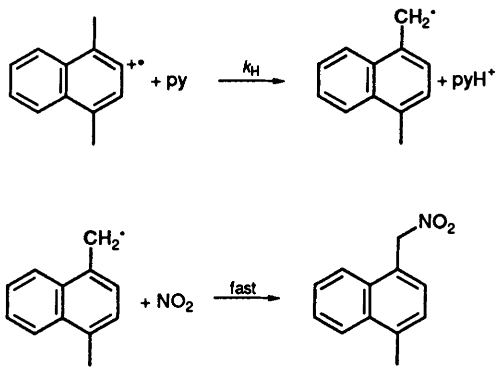

(27)

(28)

Scheme 6

Since the values of k_H in Table 3 relate to the sidechain deprotonation of DMN$^{+•}$, the resultant production of the benzylic radical provides the most direct pathway for sidechain nitration to occur, *i.e.*, Scheme 6. According to Scheme 6, the aromatic products derive from a rapid, subsequent reaction of the alkyl radical with NO$_2$ [eqn. (28)], which represents a facile, homolytic coupling with little or no activation energy.[40] The deprotonation of DMN$^{+•}$ in this way, coupled with the charge-transfer activation of the tetranitromethane complex (Scheme 2), accounts for the overall stoichiometry in eqn. (25). The spectral observation of the 1,4-dimethylnaphthalene cation radical, and its unambiguous pseudo-first-order decay in the presence of various pyridines, thus establish the efficacy with which the added bases are able to deprotonate DMN$^{+•}$ on its way to sidechain nitration [eqn. (25)]. The question then arises as to the charge-transfer nitration of DMN in the *absence* of added bases. The study of the deuterium kinetic isotope effect again helps to identify how the reactive triads formed in Schemes 2 and 3 decay to products. Thus the observed second-order decay of the spectral transient in dichloromethane occurred with the same rate constant, $k_2 = 2.1 \times 10^7$ A^{-1} s^{-1}, when 1,4-dimethylnaphthalene was replaced with its hexadeuterio derivative [$^2H_6$]DMN. The absence of a kinetic isotope effect thus supports the direct collapse of the reactive triad to the *ipso* adduct as formulated in Scheme 4. Similarly, the small KIE of $k_H/k_D = 1.1$ for the charge-transfer nitration in acetonitrile suggests that the low yield of the product of sidechain nitration in eqn. (14) derives from a minor competition from the deprotonation of DMN$^{+•}$ by the accompanying trinitromethanide anion, as established in the earlier study.[35] This formulation is supported by the observation of $k_H/k_D = 1.3$ for the charge-transfer activation of the *N*-nitropyridinium complex with DMN in acetonitrile. Thus the observation of the sidechain product in *ca.* 30% yield in Table 2 (entry 5) is consistent with the deprotonation of DMN$^{+•}$ by the pyridine present within the triad (Scheme 3), occurring with the same KIE as that effected by added base (Scheme 6).

Experimental

Materials.—Naphthalene (Matheson, Coleman & Bell) was recrystallized from ethanol and then sublimed *in vacuo*. 1,4-Dimethylnaphthalene (Aldrich) was used as received. 1,4-Di[$^2H_3$]methylnaphthalene was prepared by the methylation of 1,4-dibromonaphthalene using n-butyllithium (Aldrich) and [$^2H_3$]iodomethane (Aldrich, 99+ atom%) according to literature procedure.[34] It was purified by vacuum distillation. The ^{1}H NMR spectrum of the distilled sample was identical with that of 1,4-dimethylnaphthalene except that the singlet resonance for the methyl groups was absent. δ_H(CDCl$_3$) 7.98 (m, 2 H), 7.49 (m, 2 H) and 7.18 (s, 2 H); *m*/*z* (EI, 70 eV): 163 (13), 162 (100, M$^+$), 161 (18), 160 (16), 146 (11), 145 (35), 144 (82), 118 (12) and 117 (11). 1,4-Dibromonaphthalene was prepared by the bromination of naphthalene with dioxane dibromide according to a literature procedure.[41] Tetra-n-butylammonium trinitromethanide,[42] tetranitromethane[43] and *N*-nitropyridinium tetrafluoroborate[44] were prepared according to literature procedures. Lithium perchlorate and tetra-n-butylammonium perchlorate (G. F. Smith) were recrystallized from a mixture of acetonitrile and ethyl acetate and dried over P$_2$O$_5$ *in vacuo*. Acetonitrile (Fisher HPLC grade) and dichloromethane (Fisher) were distilled from P$_2$O$_5$ and stored in Schlenk flasks under an argon atmosphere.

Instrumentation.—The electronic spectra were recorded on a Hewlett-Packard 8450A diode array spectrometer. NMR spectra were recorded on a JEOL FX90Q spectrometer operating at 90 MHz for ^1H. The chemical shifts are reported in ppm downfield from an Me_4Si internal standard. The gas chromatographic analyses were performed on a Hewlett-Packard 5790A chromatograph using a 12.5 M SE-30 (cross-linked methylsilicone) capillary column. The GC–MS analyses were carried out on a Hewlett-Packard 5890 chromatograph interfaced to a HP5970 mass spectrometer (EI, 70 eV). Steady-state photochemical irradiations were performed with a focussed beam from either a 450 W xenon lamp (Osram, XBO-450W OFR) or a 500 W mercury lamp (Osram, HBO-2L2). The light passed through an IR water filter coupled to a Corning CS-3-72 ($\lambda < 425$ nm) glass cut-off filter. Irradiations were performed in a 1 cm quartz cell immersed in cold water contained in a Pyrex Dewar.

Time-resolved Absorption Spectra and the Decay of the Spectral Transients.—Time-resolved differential absorption spectra of the transient intermediates were obtained on a laser-flash system. The 532 nm (second harmonic) pulse from a Quantel YG 581 laser (pulse width 11 ns, Q-switched) was used, together with probe assemblies consisting of a 150 W Xe lamp, SPEX minimate monochromator, Hamamatsu R928 NM photomultiplier, and a Biomation 8100 waveform recorder or a Tektronix R7912 digitizer.[45] Digitized signals were averaged and analysed on a PDP 11/70 computer.[46] The laser intensity was attenuated with wire-mesh filters (4–100% transmittance) in order to moderate the concentration of the transients. The latter was especially important to test the validity of the second-order kinetics. For each experiment, ten shots were averaged to obtain the decay curves. The kinetic order for the decay was established by a linear least-squares computer fit of the observed decrease of absorbance (A) with time as a function of either ln (A) or A^{-1} for first- and second-order, respectively. The decay kinetics and the kinetic isotope effect were measured on a laser flash system consisting of a Quantel YG580-10 Q-switched Nd^{3+}:YAG laser with a pulse width of 10 ns (fwhm). The 1064 nm pulse was frequency doubled with a KDP crystal and separated from the residual 1064 nm beam with a dichroic mirror to obtain 532 nm pulses of 160–170 mJ per shot. The laser intensity was attenuated using wire-mesh filters (50 and 30% transmittance, with energy outputs of 75 and 50 mJ, respectively, at 532 nm). The probe beam consisted of the output from a 150 W xenon lamp in an Oriel lamp housing with an Aspherab UV-grade condensing lens. The probe beam was focussed onto the sample, and then the emerging beam from the sample was focussed onto an Oriel 77250 monochromator. A Hamamatsu R928NM photomultiplier tube attached to the exit slit of the monochromator served as the detector. The timing of the sequence for the excitation and probing of the sample was controlled by a Kinetic Instruments sequence generator and laser controller. Data acquisition and digitization were performed with a Tektronix 7104 oscilloscope in conjunction with a Tektronix C101 video camera and Tektronix DCSO1 software. The data processing employed an AT&T 6300-plus computer using the ASYST 2.0 software.

Time-resolved differential absorption spectra in the picosecond timescale were obtained using a laser-flash system that utilized the 532 nm (second harmonic), 30 ps (fwhm) pulses from a Quantel YG 402 mode-locked Nd:YAG laser as the excitation source.[47] The analysing beam was produced by passing the fundamental (1064 nm) through a solution consisting of a 1:1 mixture (v/v) of D_2O and H_2O in a 10 cm cuvette to generate a pulse of white light. Temporal measurements were made by varying the path length of the second harmonic with respect to the fundamental. The spectrograph was calibrated using the 532 nm band of the excitation pulse as well as the 436 and 546 nm lines from a mercury calibration lamp. Spectra were measured at various delay times and 30 individual pulses were averaged at each time setting.

Salt Effect on the Decay of $(DMN)_2^{+\bullet}$ *in* CH_2Cl_2.—The effect of added salt on the second order decay kinetics of $(DMN)_2^{+\bullet}$ in CH_2Cl_2 was examined using tetra-n-butylammonium perchlorate (TBAP) as the inert salt and tetra-n-butylammonium trinitromethanide (TBAT) as the common salt. A solution containing 0.05 mol dm^{-3} 1,4-dimethylnaphthalene, 0.16 mol dm^{-3} tetranitromethane and the salt in CH_2Cl_2 (2 cm^3) was irradiated at 532 nm. The decay of the $(DMN)_2^{+\bullet}$ was monitored at 625 nm. In the presence of TBAP (0.08 to 0.2 mol dm^{-3}) the decay kinetics were second order and in the presence of TBAT (0.05 and 0.1 mol dm^{-3}) the decay kinetics were first order. The kinetics were unaffected by changes in the laser intensity.

Time-resolved Absorption Spectra and the Decay of the Spectral Transients from the N-*nitropyridinium Complexes.*—The transient absorption spectra were obtained by the excitation of a solution containing 0.05 mol dm^{-3} arene and 0.1 mol dm^{-3} $pyNO_2BF_2$ in acetonitrile, using the 532 nm second harmonic pulse from a Nd:YAG laser, in a 1 cm quartz cell fitted with a Teflon stopcock. The solutions were prepared and kept under a dry nitrogen atmosphere during the experiment. After obtaining the transient absorption spectra, the decay kinetics were followed at the absorption maxima. The decay of the radical cations from hexamethylbenzene, 1,4-dimethylnaphthalene, 9-methylanthracene and 9,10-dimethylanthracene all followed first-order kinetics.

Pulse Radiolytic Generation of $(DMN)_2^{+\bullet}$.—The radical cation $(DMN)_2^{+\bullet}$ was produced by pulse radiolysis using $SO_4^{-\bullet}$ as the oxidant in aqueous acidic solution. A van de Graaff type electron generator delivering single 800 ns pulses of $\approx$4 MeV electrons with a dose rate of 50 rad ns^{-1} A^{-1} was used as the electron source. A 150 W xenon lamp was used as the monitor. A Spex Minimate monochromator, a Hamamatsu R928 photomultiplier tube and a Tektronix R7912 digitizer were used for the probe assembly. The probe assembly was interfaced with a Digital Equipment PDP 11/70 computer for analysis of the data.

In pulse radiolysis experiments the water used was distilled from potassium permanganate. A stock solution containing 10^{-3} mol dm^{-3} potassium persulphate was prepared and the pH was adjusted to 2.4 by addition of perchloric acid. The solution was saturated with DMN by addition of an excess of DMN and sonication of the solution for 10 min. Then the solution was saturated with N_2O by bubbling N_2O gas through it for 15 min. In a typical experiment 30 cm^3 of an aqueous solution, containing 10^{-3} mol dm^{-3} $K_2S_2O_8$ and saturated with DMN and N_2O, was taken in a hypodermic syringe. The syringe was attached to a flow cell (1 cm path length). Fresh solution was injected into the cell after each pulse of electrons. The differential absorption spectrum of the dimer radical cation of DMN was obtained by scanning from 300 to 800 nm at 10 nm intervals. The $(DMN)_2^{+\bullet}$ spectrum obtained by this method had λ_{max} at 380, 430sh, 660, 690 and 720 nm.

Charge-transfer Nitration of DMN Complexes in Acetonitrile.—The actinic irradiation of the charge-transfer complex of 1,4-dimethylnaphthalene with the tetranitromethane and *N*-nitropyridinium acceptors was carried out in acetonitrile solution, as described previously.[1] Typically the charge-transfer nitrations with added pyridine bases were carried out as follows. A solution containing 1,4-dimethylnaphthalene (46 mm^3, 0.3 mmol), TNM (100 mm^3, 0.8 mmol) and 2,6-di-t-butylpyridine

(57 mg, 0.3 mmol) in acetonitrile (3 cm^3) was irradiated at 0 °C using visible light ($\lambda > 425$ nm) for 3.5 h. The reaction mixture was diluted with ether and extracted with water, to remove the nitroform formed, until the aqueous extract was colourless. The yield of nitroform was 0.28 mmol (86%) based on the spectrophotometric determination. The organic layer was dried over anhydrous $MgSO_4$ and solvent was removed. The resulting yellow oil contained 4-methyl-1-nitromethylnaphthalene (62%), 1,4-dimethyl-2-nitronaphthalene (13%) and the photoadduct (9%), based on the ^{1}H NMR spectral studies using CH_3NO_2 as the internal standard. A blank experiment under identical conditions, but in the absence of 1,4-dimethylnaphthalene, yielded only 4% nitroform after irradiation for 3.5 h. Thus the decomposition of TNM by 2,6-di-t-butylpyridine was very slow under the reaction conditions. In another experiment a solution containing 1,4-dimethylnaphthalene (46 mm^3, 0.3 mmol), TNM (180 mm^3, 1.5 mmol) and 2,4,6-trimethylpyridine (36 mg, 0.3 mmol) in acetonitrile (3 cm^3) was irradiated at 0 °C for 5 h to yield 4-methyl-1-nitromethylnaphthalene (44%) and 1,4-dimethyl-2-nitronaphthalene (10%), together with recovered 1,4-dimethylnaphthalene (46%).

Kinetics of the Deprotonation of $(DMN)_2^{+\bullet}$ *by Substituted Pyridine Bases.*—The kinetics of decay of $(DMN)_2^{+\bullet}$ by lutidine, collidine and 2,6-di-t-butylpyridine were followed subsequent to the excitation, at 532 nm, of solutions containing 0.05 mol dm^{-3} DMN and 0.1 mol dm^{-3} TNM in CH_2Cl_2 and CH_3CN. The concentrations of lutidine and collidine were varied from 0.025 mol dm^{-3} to 0.128 mol dm^{-3} and that of 2,6-di-t-butylpyridine from 0.009 to 0.11 mol dm^{-3}. The decay kinetics were followed at 650 nm. In both solvents the decay of $(DMN)_2^{+\bullet}$ followed clean first-order kinetics, and the rate constants were unaffected by variation of the laser pulse intensity. The rate constants for the deprotonation determined under pseudo-first-order conditions (with a large excess of base) are listed in Table 3.

Kinetic Isotope Effect for the Deprotonation of $(DMN)_2^{+\bullet}$ *by 2,4,6-Collidine.*—The decay kinetics of $(DMN)_2^{+\bullet}$ and $([^2H_6]DMN)_2^{+\bullet}$ in the presence of an excess of collidine, in CH_2Cl_2 and CH_3CN, were followed after excitation of solutions containing 0.05 mol dm^{-3} DMN or $[^2H_6]$DMN and 0.1 mol dm^{-3} TNM. The concentration of collidine was varied from 0.025 to 0.128 mol dm^{-3}. The decay at 650 nm followed first-order kinetics. The first-order rate constant increased linearly ($r = 0.99$) with increasing concentration of the base. The deprotonation rate constants were obtained from the slope of the linear plots. In CH_2Cl_2 $k_H = 5.9 \times 10^6$ mol^{-1} dm^3 s^{-1}, $k_D = 1.4 \times 10^6$ mol^{-1} dm^3 s^{-1} and $k_H/k_D = 4.2$; in CH_3CN $k_H = 2.7 \times 10^6$ mol^{-1} dm^3 s^{-1}, $k_D = 0.58 \times 10^6$ mol^{-1} dm^3 s^{-1} and $k_H/k_D = 4.6$.

Acknowledgements

We thank the Center for Fast Kinetics Research for use of their van de Graaf generator, S. J. Atherton for helpful advice, the National Science Foundation for funds to construct the laser-flash (ps and ns–µs) photolysis apparatus, and the Robert A. Welch Foundation and the Texas Advanced Research Project for financial assistance.

References

1 S. Sankararaman and J. K. Kochi, *J. Chem. Soc., Perkin Trans. 2*, 1991, 1.
2 A. Fischer and F. Wilkinson, *Can. J. Chem.*, 1972, **50**, 3988.
3 See K. Schofield, in *Aromatic Nitration*, Cambridge University Press, New York, 1980.
4 L. Eberson and F. Radner, *Acc. Chem. Res.*, 1987, **20**, 53; Z. V. Todres, *Russ. Chem. Rev. (Engl. Transl.)*, 1978, **47**, 148; Z. V. Todres, *Tetrahedron*, 1985, **41**, 2771.
5 S. Sankararaman, W. A. Haney and J. K. Kochi, *J. Am. Chem. Soc.*, 1987, **109**, 5235.
6 S. Sankararaman, W. A. Haney and J. K. Kochi, *J. Am. Chem. Soc.*, 1987, **109**, 7824.
7 J. M. Masnovi, J. K. Kochi, E. F. Hilinski and P. M. Rentzepis, *J. Am. Chem. Soc.*, 1986, **108**, 1126.
8 K. Y. Lee, unpublished results.
9 H. A. Benesi and J. H. Hildebrand, *J. Am. Chem. Soc.*, 1949, **71**, 2703; W. B. Person, *J. Am. Chem. Soc.*, 1965, **87**, 167.
10 R. S. Mulliken, *J. Am. Chem. Soc.*, 1952, **74**, 811.
11 R. S. Mulliken and W. B. Person, *Molecular Complexes*, A Lecture and Reprint Volume, Wiley, New York, 1969.
12 R. A. Friedel and M. Orchin, *Ultraviolet Spectra of Aromatic Compounds*, Wiley, New York, 1951.
13 K. V. Altukhov and V. V. Perekalin, *Russ. Chem. Rev.*, 1976, **45**, 1052.
14 Y. Takahashi, S. Sankararaman and J. K. Kochi, *J. Am. Chem. Soc.*, 1989, **111**, 2954.
15 J. M. Wallis and J. K. Kochi, *J. Am. Chem. Soc.*, 1988, **110**, 8207.
16 B. Badger and B. Brocklehurst, *Trans. Faraday Soc.*, 1969, **65**, 2588; B. Brocklehurst and R. D. Russell, *Trans. Faraday Soc.*, 1969, **65**, 2159; B. Badger, B. Brocklehurst and R. D. Russell, *Chem. Phys. Lett.*, 1967, **1**, 122.
17 S. Steenken, C. J. Warren and B. C. Gilbert, *J. Chem. Soc., Perkin Trans. 2*, 1990, 335.
18 P. O'Neill, S. Steenken and D. Schulte-Frohlinde, *J. Phys. Chem.*, 1975, **79**, 2773; K. Sehestad and J. Holcman, *J. Phys. Chem.*, 1978, **82**, 651.
19 A. Kira and M. Imamura, *J. Phys. Chem.*, 1979, **83**, 2267; A. Kira, M. Imamura and T. Shida, *J. Phys. Chem.*, 1976, **80**, 1445; A. Kira, T. Nakamura and M. Imamura, *J. Phys. Chem.*, 1977, **81**, 511.
20 T. Shida and W. H. Hamill, *J. Chem. Phys.*, 1966, **44**, 2375, 4372.
21 R. Gschwind and E. Haselbach, *Helv. Chim. Acta*, 1979, **97**, 941.
22 J. M. Masnovi, E. F. Hilinski, P. M. Rentzepis and J. K. Kochi, *J. Phys. Chem.*, 1985, **89**, 5387.
23 J. M. Masnovi and J. K. Kochi, *J. Phys. Chem.*, 1987, **91**, 1878.
24 G. D. Gillespie and A. U. Khan, *J. Chem. Phys.*, 1976, **65**, 1624; T. C. Hall, Jr. and F. E. Blacet, *J. Chem. Phys.*, 1952, **20**, 1745.
25 W. Lau and J. K. Kochi, *J. Am. Chem. Soc.*, 1984, **106**, 7100; *J. Org. Chem.*, 1986, **31**, 1801.
26 J. M. Masnovi, E. A. Seddon and J. K. Kochi, *Can. J. Chem.*, 1984, **62**, 2552.
27 Compare also M. A. J. Rodgers, *Trans. Faraday Soc.*, 1971, **67**, 1029.
28 J. M. Masnovi, A. Levine and J. K. Kochi, *J. Am. Chem. Soc.*, 1985, **107**, 4356.
29 J. M. Masnovi and J. K. Kochi, *J. Am. Chem. Soc.*, 1985, **107**, 7880.
30 K. K. Sharma and R. J. Boyd, *Theor. Chim. Acta*, 1979, **53**, 309.
31 J. E. Gordon, *Organic Chemistry of Electrolyte Solutions*, Wiley, New York, 1975.
32 *Ions and Ion Pairs in Organic Reactions*, ed. M. Szwarc, Wiley, New York, 1972–1974, vols. 1 and 2.
33 T. M. Bockman and J. K. Kochi, *J. Am. Chem. Soc.*, 1988, **110**, 1294; T. M. Bockman and J. K. Kochi, *J. Am. Chem. Soc.*, 1989, **111**, 4669.
34 P. Diabo, M. F. Mouneyrac, B. Pasquier-Chenon and L. C. Leitch, *J. Labelled Compd.*, 1966, II, 272.
35 J. M. Masnovi, S. Sankararaman and J. K. Kochi, *J. Am. Chem. Soc.*, 1989, **111**, 2263.
36 C. J. Schlesener, C. Amatore and J. K. Kochi, *J. Am. Chem. Soc.*, 1984, **106**, 7472.
37 C. Amatore, personal communication.
38 S. Sankararaman, unpublished results.
39 J. O. Howell, J. M. Goncalves, C. Amatore, L. Klasinc, R. M. Wightman and J. K. Kochi, *J. Am. Chem. Soc.*, 1984, **106**, 3968.
40 D. H. Giamalva, G. B. Kenion, D. F. Church and W. A. Pryor, *J. Am. Chem. Soc.*, 1987, **109**, 7059.
41 R. W. Bayer and E. J. O'Reilly, Jr., *J. Org. Chem.*, 1958, **23**, 311.
42 J. M. Masnovi and J. K. Kochi, *J. Org. Chem.*, 1985, **50**, 5245.
43 P. Liang, *Org. Synth.*, Coll. Vol. III, 1955, 803.
44 G. A. Olah, J. A. Olah and N. A. Overchuk, *J. Org. Chem.*, 1965, **30**, 3373.
45 S. J. Atherton, *J. Phys. Chem.*, 1984, **88**, 2840.
46 D. C. Foyt, *J. Comput. Chem.*, 1981, **5**, 49.
47 S. J. Atherton, S. M. Hubig, T. J. Callan, J. A. Duncanson, P. T. Snowden and M. A. J. Rodgers, *J. Phys. Chem.*, 1987, **91**, 3137.

Paper 0/03881D
Received 28*th August* 1990
Accepted 2*nd October* 1990